

This is the peer reviewed version of the following article: Anderson, C. J., Tay, W. T., McGaughran, A., Gordon, K. and Walsh, T. K. (2016), Population structure and gene flow in the global pest, *Helicoverpa armigera*. *Molecular Ecology*, 25: 5296–5311. doi: 10.1111/mec.13841, which has been published in final form at <http://doi.org/10.1111/mec.13841>. This article may be used for non-commercial purposes in accordance With Wiley Terms and Conditions for self-archiving.

**Population structure and gene flow in the global pest,
*Helicoverpa armigera***

Journal:	<i>Molecular Ecology</i>
Manuscript ID	MEC-16-0531
Manuscript Type:	Original Article
Date Submitted by the Author:	05-May-2016
Complete List of Authors:	Anderson, Craig; University of Stirling, BES; CSIRO Tay, Wee Tek; CSIRO Mcgaughran, Angela; CSIRO; University of Melbourne, School of BioSciences Gordon, Karl; CSIRO Walsh, Tom; CSIRO
Keywords:	Hybridization, Insects, Invasive Species, Population Genetics - Empirical, Ecological Genetics

1 **Population structure and gene flow in the global pest, *Helicoverpa armigera***

2

3 Anderson, C.J.^{1,2*}, Tay, W.T.², McGaughran, A.^{2,3}, Gordon, K.², Walsh, T.K.².

4 1. Biological and Environmental Sciences, University of Stirling, Stirling, FK9 4LA, UK.

5 2. CSIRO, Black Mountain Laboratories, Acton, ACT, 2601, Australia.

6 3. University of Melbourne, School of BioSciences, Melbourne, VIC, 3010, Australia.

7 Keywords: population genomics, gene flow, pest, moth, GBS

8 *Corresponding author. Email: Craig.Anderson@stir.ac.uk

9 Running title: Population structure in the pest, *H. armigera*

10

11

12

13

14

15

16

17

18

19

20

21

22

23

24 Abstract

25 *Helicoverpa armigera* is a major agricultural pest that presents a wide distribution across much of the
26 Old World. This species is hypothesised to have spread to the New World 1.5 million years ago,
27 founding a population that is at present a distinct species called *Helicoverpa zea*. In 2013, *H.*
28 *armigera* was found to have re-entered South America via Brazil and subsequently spread
29 throughout the continent. The source of the recent incursion is unknown and population structure in
30 *H. armigera* is poorly resolved, but a basic understanding would highlight potential biosecurity
31 failures and determine the recent evolutionary history of region specific lineages. Here, we integrate
32 several end points derived from high-throughput sequencing to assess gene flow in *H. armigera* and
33 *H. zea* from populations across six continents. We first assemble mitochondrial genomes to
34 demonstrate the phylogenetic relationship of *H. armigera* with other Heliiothine species, as well as
35 the lack of distinction between populations. We subsequently use *de novo* genotyping by sequencing
36 and whole genome sequences, aligned to bacterial artificial chromosomes, to assess levels of
37 admixture. Primarily, we find that European individuals are most similar to Brazilian *H. armigera* and
38 also identify a potential hybrid between *H. armigera* and *H. zea*. We also demonstrate the
39 occurrence of an *H. armigera* subspecies that is generally endemic to Australia. While structure
40 among the bulk of populations remains unresolved, we present distinctions that are pertinent to
41 future investigations as well as to the biosecurity threat posed by *H. armigera*.

42 Introduction

43 Identifying population structure and patterns of gene flow in any species is often the basis for
44 understanding the complexities of current and historical relationships (Martin *et al.* 2013;
45 Nadachowska-Brzyska *et al.* 2013; Sankararaman *et al.* 2014). This information can have a number of
46 important implications for conservation, management of invasive species and predicting the spread
47 of novel phenotypes within a species distribution (Kirk *et al.* 2013; Prado-Martinez *et al.* 2013;

48 Malinsky *et al.* 2015). For example, one phenotype that can spread through populations is resistance
49 to pesticides and understanding the population genetic factors underpinning this process can help to
50 predict the spread and minimise damage imposed by pest species presenting this unwanted
51 phenotype (Jin *et al.* 2015).

52 *Helicoverpa armigera* is one of the most significant pests of agriculture, with a wide range of suitable
53 hosts and climatic conditions, rapid rates of reproduction, and a capacity for long distance dispersal
54 across its largely Old World distribution (Fitt 1989; McCaffery 1998; Feng *et al.* 2005). Recent
55 modelling work has identified that the potential value of crops exposed to *H. armigera* totals
56 approximately US \$78 billion p.a. (Kriticos *et al.* 2015). Though *H. armigera* has typically been
57 confined to the Old World (Europe, Africa, Asia and Australasia), it was identified in Brazil in 2013,
58 before subsequently being identified as far north as Puerto Rico (2014) and Florida (2015) (Tay *et al.*
59 2013; Czepak *et al.* 2013; Hayden & Brambila 2015; Kriticos *et al.* 2015). The New World is typically
60 the range of a closely related species, *Helicoverpa zea*, which is hypothesised to be the product of an
61 ancient incursion by *H. armigera* approximately 1.5-2 million years ago (Behere *et al.* 2007). The two
62 species are capable of hybridising in the laboratory (Hardwick 1965), however natural occurrences
63 have yet to be recorded (Laster & Sheng 1995; Laster & Hardee 1995).

64 Previous work aiming to identify genetic variation with insight into population structure has lacked
65 resolution in *H. armigera*. Mitochondrial markers are capable of determining variation at the species
66 level and have been used, sometimes in tandem with genomic markers, in an attempt to distinguish
67 populations. Taxonomic characterisation of two *H. armigera* strains has highlighted a potential
68 distinction between Australian populations (*H. armigera conferta*) and the "Rest of the world" (*H.*
69 *armigera armigera*) (Matthews 1999). However, much research (discussed in Behere *et al.* (2013))
70 has shown limited evidence of consistent structure on local or global scale.

71 Genetic variation derived from recent selection events can be useful for inferring population
72 structure over regional scales and in turn, effectively allow for the inference of associated
73 phenotypes. Where pesticides have been widely implemented to control *H. armigera*, resistance has
74 been selected for and spread rapidly through populations in response to a broad range of treatments
75 (Gunning *et al.* 2005; Yang *et al.* 2013; Tay *et al.* 2015). Of the many cases of resistance, that among
76 populations of *H. armigera* to the pyrethroid, fenvalerate, has been particularly well studied.
77 Introduced in the late 1970s, resistance to fenvalerate became established in Australia within six
78 years and is now extremely common around the world (McCaffery 1998). The mechanism was
79 identified as a chimeric P450, *CYP337B3* (Joußen *et al.* 2012), and subsequent analysis has identified
80 a number of different haplotypes associated with geographic localities that imply independent
81 evolutionary events and should be useful for inferring population structure (Walsh *et al.* submitted;
82 Joußen *et al.* 2012; Rasool *et al.* 2014).

83 Recently developed molecular methods have been used to increase ability to identify population
84 structure by massively increasing the number of markers available for analysis (Andrews *et al.* 2016).
85 In particular, genotyping by sequencing (GBS) methods such as restriction associated DNA
86 sequencing (RADseq), offer a powerful means for identifying genetic variation associated with
87 specific phenotypes (Davey *et al.* 2011). These data, especially when mapped to a reference genome,
88 have proven to be capable of identifying candidate genotype-phenotype associations and are
89 underpinned by a series of increasingly sophisticated analytical tools (Patterson *et al.* 2006; Falush *et*
90 *al.* 2007; Allendorf *et al.* 2010; Catchen *et al.* 2013b; Sousa & Hey 2013; Veeramah & Hammer 2014).

91 Given the technological developments within the field of molecular ecology, and in light of recent
92 developments concerning the spread of *H. armigera*, we have used contemporary sequencing
93 methods in an attempt to resolve *H. armigera* population structure and gene flow across the globe.
94 We use high-throughput sequencing data for *H. armigera* and several other Heliothine species to

95 confirm the phylogenetic relationship between species and populations through whole mitochondrial
96 genome sequencing. We subsequently use *de novo* GBS to determine population structure and gene
97 flow at a continental scale in *H. armigera* and *H. zea*. Finally, we use publically available bacterial
98 artificial chromosome (BAC) sequences to determine possible signals of gene flow, population
99 structure and other evolutionary processes that can be inferred from across 20 BACs (approximately
100 2.3 Mb of the genome), including the region where the locus involved in fenvalorate resistance,
101 *CYP337B3*, is found. Overall, this work offers insights into the potential sources of recent *H. armigera*
102 incursions into Brazil, as well as describing global population structure in *H. armigera* and evidence of
103 hybridisation among *H. armigera* and *H. zea*.

104 **Methods**

105 *Sample collection and DNA extraction*

106 Heliothine moths, including *H. armigera*, were collected between 2007 and 2014 from 16 different
107 countries around the world across various climatic zones and altitudes (Tables S1 and S2), many of
108 which are described in Behere *et al.* (2007); and Tay *et al.* (2013). Samples were collected as larvae
109 from wild and crop host plants, as adult moths via light/pheromone traps, or as larvae after bioassay,
110 and preserved in ethanol (>95%) or RNAlater, or stored at -20°C prior to DNA extraction. DNA was
111 extracted from samples using DNeasy blood and tissue kits (Qiagen), before being quantified with a
112 Qubit 2.0.

113 *Species Identification*

114 The species status of several preserved specimens was confirmed by mitochondrial gene (COI and
115 Cytb) sequencing, either from previous work (Walsh *et al.* submitted ; Behere *et al.* 2007; Tay *et al.*
116 2013,) or, where new samples were available, by amplifying and sequencing the same regions. PCR
117 amplification followed the protocols of Behere *et al.* (2007) and Tay *et al.* (2013), using the primers

118 Harm-COI-F02/R02 and Harm-Cytb-F02/R02. PCR products were sequenced at Macrogen (Seoul,
119 Korea) and the Biological Resources Facility (Australian National University, Canberra, Australia).
120 Assembly of DNA trace sequences was performed using CLC Genomics Workbench v. 8.0
121 (www.clcbio.com).

122 *Genotyping by Sequencing*

123 GBS library preparation and sequencing was outsourced to Cornell University. Information regarding
124 the samples used and sequencing output is recorded in the supplementary material (Table S1).
125 Briefly, 50 ng of gDNA was digested using PstI, before being sequenced using an Illumina HiSeq. A
126 negative control was included with each plate. Raw data were assessed for quality and processed
127 using Stacks v. 1.30 (Catchen *et al.* 2013b). Briefly, `process_radtags` was used to demultiplex samples,
128 trim to 90 bp and assess the quality of reads before being forwarded to `denovo_map`, which was run
129 using default settings. The Populations module was then run, limiting the output to loci existing in at
130 least 5% of the population with at least 5x coverage. The Populations module was used to output
131 SNP data in Plink and Structure formats, the latter of which was limited to handling a single SNP per
132 locus, chosen at random to account for linkage. Population level statistics were calculated using the
133 Populations module and included pairwise F_{ST} , which was summarised using PCA conducted in
134 Minitab v. 1.7 (www.minitab.com). Minitab was also used to calculate Pearson's correlation
135 coefficient between principle components and missing data. For these analyses, two discrete
136 samples of *H. zea* were defined based on their sample collection date being either putatively before
137 or after the invasion of *H. armigera* (denoted as "Brazil zea" and "Brazil zea 2", respectively).

138 *Whole Genome Sequencing*

139 Nextera libraries were produced following the manufacturer's instructions and sequence was
140 generated as 100 bp PE reads (Illumina HiSeq 2000, Biological Resources Facility, Australian National

141 University, Canberra, Australia, as well as at Beijing Genomics Institute, Hong Kong). Sample and
142 sequencing data are included in the supplementary material.

143 *Mitochondrial genome assembly and analysis*

144 Raw sequence reads obtained from whole genome sequencing were aligned to the *H. armigera*
145 mitochondrial genome using BMAP v. 33.43 (<http://sourceforge.net/projects/bbmap/>), permitting a
146 minimum identity of 0.6 and allowing for a minimum quality threshold equivalent to Q10 over two
147 consecutive bases before reads were trimmed. Reads were assembled using mira v. 4 (Chevreux *et*
148 *al.* 2004) before mitobim v. 1.7 (Hahn *et al.* 2013) was used to iteratively map and assemble whole
149 mitochondrial sequences. Heterozygous bases were removed, sequences were aligned using MAFFT
150 v. 7.017 (Kato 2002) and sequences were trimmed using the Gblocks v. 0.91b online server
151 (http://molevol.cmima.csic.es/castresana/Gblocks_server.html) (Talavera & Castresana 2007).

152 Statistical selection of nucleotide substitution models were estimated using jModelTest and the SYM
153 model was implemented. A phylogenetic tree was then estimated using MrBayes v. 3.2.2 (Ronquist &
154 Huelsenbeck 2003) via Geneious v. 8.1.7 (www.geneious.com), using a GTR substitution model as
155 identified in jModelTest v. 2.1.7 (Posada 2008). Run parameters were: a chain length of 1,100,000
156 and a burn-in length of 100,000 over 4 heated-chains (chain temp 0.2). Pairwise nucleotide distance
157 between species was measured using default parameters in MEGA v. 6.0 (Tamura *et al.* 2013). A
158 haplotype network was calculated and generated using Popart v. 1.7 (Forster & Ro 1994; Leigh &
159 Bryant 2015). Mitochondrial variants were then used to test for genetic divergence through
160 calculation of pairwise differences for Φ_{st} (a measure related to F_{ST} used for haplotype data) using
161 Arlequin v. 3.5.2.2 (Excoffier *et al.* 1992), with significance assessed using 20,000 permutations.
162 Geographic structure among populations was also tested in Arlequin, using analysis of molecular
163 variance (AMOVA).

164 *Alignment and processing of whole genome sequencing data*

165 Raw reads were aligned to BAC sequences, originally derived from *H. armigera* and available on NCBI
166 (accessions in supplementary document), using BMAP. Reads were trimmed when quality in at least
167 2 bases fell below Q10. Only uniquely aligning reads were included in the analysis, to prevent
168 spuriously inferring evolutionary processes occurring independently on each BAC. Outputted BAM
169 files were sorted before duplicate reads were removed and files were annotated with read groups
170 using Picard v. 1.138 (<http://picard.sourceforge.net>). BAC reference sequences were indexed using
171 Samtools v. 1.1.0 (Li *et al.* 2009). UnifiedGenotyper in GATK v. 3.3-0 (McKenna *et al.* 2010) was used
172 to estimate genotypes across all individuals simultaneously, implementing a heterozygosity value of
173 0.01. Variant call format files containing SNP calls were reformatted into Plink format using VCFtools
174 v. 0.1.12b (Danecek *et al.* 2011). When linkage disequilibrium (LD)-based pruning was necessary,
175 Plink v. 1.07 (Purcell *et al.* 2007) was used to filter one of a pair of SNPs using a pairwise LD threshold
176 ($r^2=0.5$) within windows of 50 SNPs, moving forwards 5 SNPs per iteration.

177 *Structure Analysis*

178 The software, Structure v. 2.3.4 (Pritchard *et al.* 2000; Falush *et al.* 2007), was used on both GBS and
179 BAC data to implement a model-based clustering method for inferring population structure. For all
180 analyses, an initial run of 1,000 burn-in was followed by 1,000 repetitions of data collection, with $K =$
181 1 to estimate the allele frequency distribution (λ), where K is the assumed number of
182 populations. For the GBS data, 2,671 SNPs derived from all *H. armigera* and *H. zea* populations were
183 tested across runs (20,000 burn-in, 20,000 data collection) implementing values of K from 1-5, with 8
184 replicates of each K -value, before Structure Harvester v. 0.6.94 (Earl & vonHoldt 2012) was used to
185 identify the most appropriate value of K via implementation of the Evanno method (Evanno *et al.*
186 2005). The optimal K for each analysis was implemented in a final run (100,000 burn-in, 100,000 data
187 collection) and results were plotted using Distruct2.pl (<https://github.com/crytpic0/distruct2>).
188 Separate analyses focusing on all *H. armigera* populations (6,713 loci), and then on *H. armigera*

189 without individuals from Australia (6,868 loci) were also run, testing K in the ranges of 1-5 and 1-7,
190 respectively. Structure analysis of BAC-aligned whole genome sequences was performed in a similar
191 manner, but focused only on all populations of *H. armigera* to limit computational requirements,
192 testing values of K between 1 and 7.

193 *Principle component analysis and the D statistic*

194 GBS and BAC-aligned data in Plink format was converted to eigenstrat format using the convertf
195 module from EIGENSOFT v. 6.0.1 (Patterson *et al.* 2006). SNPs generated from GBS data were
196 randomly attributed to one of 64 pseudo-chromosomes to obtain standard errors and calculate Z-
197 scores. PCA was performed using the smartPCA module, implementing the LSQ option, with no
198 automatic outlier removal allowed. A Tracy-Widom distribution was used to infer statistical
199 significance for principle components, with a threshold of 1×10^{-12} . Additionally, the “missing data”
200 option was implemented to assess patterns of population structure where genotypes are present/
201 absent in the GBS data.

202 The *D* statistic is a measure of admixture between populations that is robust to biases associated
203 with SNP ascertainment and demographic history, as well as the outlier incorporated (Patterson *et al.*
204 2012). The *D* statistic can be calculated using AdmixTools v. 3.0 (Patterson *et al.* 2012), where the
205 estimation makes use of tree-like histories (explained in detail in Durand *et al.* 2011). In this instance,
206 the program incorporates a structure of (Out group, *x*; *y*, *H. zea* (USA)), where *x* and *y* are
207 combinations of *H. armigera* populations as defined by country of origin. Under the assumptions of
208 the model, there is no assumed gene flow between the out group and *H. zea*, but there is potential
209 gene flow allowable between either *x* and *y* or *y* and *H. zea*, which results in positive or negative *D*,
210 respectively, with *D* = 0 indicating a lack of gene flow. Calculation of *D* uses biallelic SNPs and is
211 accompanied by a Z-score that is considered to be significant when greater than three times its
212 standard error. Individuals of *Helicoverpa punctigera* were included in the GBS sequencing and serve

213 as an out group for this data, though *Helicoverpa assulta* was used as the out group for the
214 resequencing data. The more recent divergence of *H. assulta* will result in capability for fulfilling the
215 tree-like model across an increased number of SNPs. This test for admixture has been demonstrated
216 to remain robust despite the use of increasingly distant out groups (Patterson *et al.* 2012).

217 *Testing for selection across the BAC containing CYP337B3*

218 Samples were screened for the presence of *CYP337B3* using the primers described in Joußen *et al.*
219 (2012) and Walsh *et al.* (submitted). Heterozygote/homozygote status was determined through
220 relevant band detection on 1.5-2% agarose gels containing 1% (w/v) of GelRed (Biotium) and
221 visualised under UV light. Sanger sequences were generated from these short fragments for a subset
222 of samples following the PCR amplification protocol of Joußen *et al.* (2012) and Walsh *et al.*
223 (submitted).

224 VCFtools was used to calculate π and Tajima's D in *CYP337B3*-positive individuals, as defined via
225 Sanger sequencing and PCA cluster membership, in sliding windows of 2,500 bp that progressed by
226 1,250 bp across biallelic sites. Results were plotted in R v. 3.1.2 (R Core Team 2014) using ggplot2 v.
227 1.0.1 (Wickham 2009), while gene annotations were derived via tblastx (Altschul *et al.* 1990) using
228 default settings, and visualised with CLC Genomics workbench v. 8.0.

229 **Results**

230 *Mitochondrial phylogeny*

231 After aligning and removing sites with missing data, 12,248 bp of the 15,539 bp full length reference
232 genome was used to infer phylogenetic relationships (Fig. 1). Phylogenetic analysis of the data
233 demonstrates that we are clearly capable of determining species-level membership of various
234 individuals included in this analysis, and faithfully follows the tree determined by Cho *et al.* (2008).
235 Pairwise distances further demonstrate the relative difference between each of the species (Table

236 S3), with both *H. armigera* from Australia and the remaining global sample registering scores of 0.03
237 and 0.05 against *H. zea* and *H. punctigera*, respectively.

238 *Inference of population structure and gene flow using mitochondrial data*

239 Calculation of the whole mitochondrial genome haplotype network (Fig. 2) shows some clustering of
240 Australian individuals in the left side of the network, however, the remaining populations are poorly
241 resolved. For example, Australian individuals also appear closer to Asian and African samples
242 throughout the network (Fig. 2). Inferences of gene flow between populations (i.e. Φ_{st} ; Table S4)
243 broadly support the haplotype network. Principle components 1 and 2 account for a total of 65.59%
244 of the variation in the data and demonstrate differentiation between *H. armigera* from Australia and
245 New Zealand from other populations (Fig. 3). In support of this, AMOVA implicated strong, significant
246 genetic structure, with 74.15% ($P < 0.00001$) of the variance apportioned among populations and
247 25.85% apportioned within (Fig. S3).

248 *Inference of population structure using de novo GBS*

249 *Principle coordinate analysis*

250 Genotyping by sequencing (GBS) data from populations of *H. armigera*, *H. zea* and *H. punctigera*
251 were used to determine if genetic variation from across the nuclear genome could provide insight
252 into population structure and gene flow. Using data from 14,548 loci, 21,043 SNPs were used to
253 reveal improved resolution in population structure and gene flow relative to mitochondrial data (Fig.
254 4). The first two eigenvalues are significant as inferred by the Tracy-Widom test ($P \leq 3.1 \times 10^{-23}$), with
255 the greatest variation (6.61%) demonstrating a distinction between *H. armigera* and *H. zea*, while the
256 second PC (1.89%), defines two discrete groups of *H. armigera*. This likely reflects *H. armigera*
257 subspecies, *H. armigera armigera* ("Rest of World") and *H. armigera conferta* (Australia), as
258 described by Matthews (1999). *H. armigera armigera* populations cannot be resolved into

259 populations using this data. Of note in Figure 4 is the presence of an individual collected in China
260 clustering among Australian *H. armigera*, as well as an individual identified by mitochondrial markers
261 as *H. zea* from Brazil that falls between the main cluster of *H. zea* and the two *H. armigera* clusters,
262 potentially representing a hybrid between the two species. When presence/absence of markers was
263 analysed using PCA, the first 6 PCs were found to be significant under the Tracy-Widom statistic ($P \leq$
264 9.57×10^{-21} , Fig. S1). Both PC1 and PC2 were negatively correlated with the amount of missing data in
265 each sample, with Pearson's correlation coefficient as -0.56 and -0.82, respectively ($P < 0.0001$).
266 Interrogation of subsequent PCs is suggestive of potential differentiation between populations,
267 though there remains a degree of overlap between *H. armigera armigera* individuals.

268 *Structure*

269 Using SNPs from the GBS analysis, the number of genetic clusters inferred by eigenstrat support the
270 Structure results (Fig. 5). Using the method established by Evanno et al. (2005), we determined that
271 $K=2$ best fit the data and clearly defined the split between *H. armigera* and *H. zea*. Expected
272 heterozygosity is a useful measure representing genetic diversity between individuals in the same
273 cluster, and in this instance was greatest in the cluster relating most to *H. armigera* (red, 0.043) over
274 that defining *H. zea* (blue, 0.020). The individual belonging to "Brazil zea 2" that was hypothesised to
275 be a hybrid between *H. armigera* and *H. zea* (see above) was found to have the highest membership
276 to the red cluster of any *H. zea* (0.367). $K=2$ was again selected following the removal of *H. zea*, but in
277 this instance, identified variation between *H. armigera armigera* (i.e., "Rest of world") and *H.*
278 *armigera conferta* (i.e., Australian *H. armigera*). Membership of Australian samples indicates a
279 relatively large degree of gene flow (i.e., where red and blue colours are present in the same bar in
280 the figure) between the two sub-species, though expected heterozygosity was greater for the cluster
281 that best defined *H. armigera armigera* (red, 0.073) over that predominantly associated with *H.*
282 *armigera conferta* (blue, 0.057). The Chinese individual found clustering with Australian *H. armigera*

283 in Figure 4 has the second highest membership towards the red (*H. armigera armigera*) cluster than
284 any other sample in this analysis. Subsequently, K=4 provided the largest delta K in an analysis of
285 populations with high membership to *H. armigera armigera*, though no cluster clearly supports
286 geographic partitioning. Expected heterozygosity is highest for cluster 4 (red) *H. armigera armigera*
287 (0.085), which represents genotypes most frequently seen among populations from China, India and
288 Uganda, at 91.2%, 83.6% and 75.6%, respectively. Brazilian individuals are most commonly found in
289 cluster 3 (blue, 52.5%), but only 22% to cluster 4 (red). Only Brazil and Uganda are frequently found
290 within cluster 2 (green).

291 *Population genetic statistics*

292 F_{ST} was calculated as corrected AMOVA F_{ST} in Stacks and is a pairwise measure across variable SNPs
293 that does not consider fixed sites (Fig. S2, Table S5). PCA demonstrates that, across PC1 (87.2%),
294 populations are clearly differentiated at a species level, with *H. armigera* from Brazil tending away
295 from other populations of *H. armigera* and towards *H. zea*; this could reflect hybridisation or similar
296 populations of origin for sampled individuals (Fig. S2). Of the other *H. armigera* populations, the
297 Australian population has the lowest observable variation in allele frequency to Brazilian *H. armigera*
298 as measured by F_{ST} . This is also emulated on PC2 (6.7%), though the reasons for the distribution
299 across PC2 are not clear. *H. zea* sampled from before and after the incursion of *H. armigera* do not
300 appear to differ extensively (Fig. S2).

301 Table 1 represents a summary of population genetic statistics derived from variant calls for samples
302 analysed using GBS markers. Nucleotide diversity (π , equivalent to expected heterozygosity) is
303 approximately the same in all *H. armigera* (including Brazil). In *H. zea*, π is lower compared to *H.*
304 *armigera* but is similar for both Brazilian populations and the population from the USA. Observed
305 heterozygosity is highest in Australia, and lower in Brazilian individuals, which present similar values
306 to all populations of *H. zea*. A positive inbreeding coefficient (F_{IS}) identifies an excess in homozygosity

307 that is indicative of genetic isolation of subpopulations by means of non-random mating or cryptic
308 population structure and recent hybridization (Catchen *et al.* 2013a). In this instance, F_{IS} is low in *H.*
309 *zea*, but higher in *H. armigera*, with the highest F_{IS} observable among Brazilian *H. armigera*. The most
310 recent sampling of *H. zea* from Brazil has higher F_{IS} , comparable with levels seen in *H. armigera*,
311 which might simply reflect the local variation. The number of private alleles, representing a basic
312 measure of genetic distinctiveness in a population, is much higher in Brazilian *H. armigera*; a more
313 geographically diverse global sample set might reduce this number, or it may be inflated due to the
314 higher number of individuals sampled relative to other populations (Kalinowski 2004).

315 *Measurement of gene flow using the D statistic*

316 21,043 SNPs were incorporated into calculation of levels of gene flow between populations via the *D*
317 statistic (Table 2). Overall, gene flow between Chinese and other populations of *H. armigera* is most
318 commonly significant under a range of tree-like scenarios. For example, *D* is most negative (-0.259)
319 under the model of (Out group, *x*; *y*, *H. zea* (USA)), when *x* is Australia and *y* is China, representing
320 gene flow between Australia and China. *D* is also negative between Chinese and Brazilian
321 populations of *H. armigera* (-0.270), though Ugandan and Indian populations appear to maintain
322 similar levels of gene flow ($D = -0.259$ and -0.251 , respectively) and appear to share similar levels of
323 gene flow with Chinese populations themselves ($D = -0.262$ and -0.237 , respectively). When
324 considering gene flow between populations of *H. zea* and Brazilian *H. armigera*, there are no
325 significant levels detected and both collections of Brazilian *H. zea* appear to be similar. *D* is only
326 significantly positive between Brazilian *H. zea* and *H. zea* from USA, and is comparable in both
327 instances tested. Furthermore, *D* is far higher in this instance than in any comparisons between *H.*
328 *armigera* populations, which is likely reflective of the population founder event that this species is
329 hypothesised to have undergone (Behere *et al.* 2007).

330 *Inference of population structure using whole genome sequencing data aligned to BACs*

331 *Principle coordinate analysis*

332 To observe the effects of increased resolution provided from alignment over BACs that accounted for
333 a total of 2.3 Mb of the *H. armigera* genome, we conducted whole genome sequencing across a
334 number of individuals representing several geographic locations (Table S2). Initially, we aligned reads
335 to all BACs deposited on NCBI, before then looking at population structure derived from a BAC
336 containing a chimeric P450 gene that is considered to be under selection (Joußen *et al.* 2012). Initial
337 insights into population specific genetic variation in all BACs were provided by PCA (Fig. 6), though
338 only PC1 was considered significant ($P=6.83 \times 10^{-48}$) and primarily reflects the distinction between *H.*
339 *armigera* and *H. zea*. A single outlier from China and two from India were manually removed from
340 this analysis after falling far from all other samples, though having been previously identified as *H.*
341 *armigera* using a mitochondrial marker. Several individuals from the geographically farthest relative
342 sampling points (Brazil, Senegal and Europe) are placed farthest from a clearly discernible Australian
343 cohort. When considering each of the BACs individually (supplementary document), this distribution
344 is maintained across several BACs, including BACs 4, 8 and 18, which most clearly define this
345 relationship. When SNPs from these three BACs are pruned to account for LD across the BACs, both
346 PC1 and PC2 are to be considered significant, with PC2 accounting for variation across *H. armigera*
347 populations ($P \leq 7.28 \times 10^{-14}$).

348 *Structure*

349 Using the method established by Evanno *et al.* (2005), we determined that K=2 best fit data for
350 analysis of population structure and defined the split between *H. armigera armigera* and *H. armigera*
351 *conferta* (Fig. 7). Expected heterozygosity is approximately similar for both cluster 1 (red) and cluster
352 2 (blue) at 0.1167 and 0.1286, respectively. Australian individuals are most clearly identified in
353 cluster 1, accounting for 84.2% of this population. While the majority of individuals from New
354 Zealand and China are placed in geographically proximal clusters, some individuals are also found to

355 have degrees of membership to cluster 1. $K=4$ also provided a notably high delta K , where certain
356 clusters are associated with specific geographic regions. Expected heterozygosity is highest for
357 cluster 3 (blue, 0.1392), which represents genotypes most frequently seen among *H. armigera*, but
358 least frequently in Chinese, Ugandan and Indian populations (25.9%, 7.1% and 1.9% respectively).
359 Cluster 1 has the next highest expected heterozygosity (yellow, 0.1358), and is most frequently found
360 among 84.2% of Indian *H. armigera* (86%). Australia and New Zealand (52.4% and 30%, respectively)
361 observe high degrees of membership to cluster 4 (red, expected heterozygosity is 0.0945), while
362 European individuals have the greatest membership to cluster 2 (green, 76.5%). Brazilian individuals
363 have the highest membership to cluster 3 (52.2%), but only 21.7% to cluster 1 and 26.1% to cluster 2
364 (Fig. 7).

365 *Population genetic statistics*

366 Values for nucleotide diversity and Tajima's D were calculated across BACs for all species sequenced
367 (Table 3, Table S6). Nucleotide diversity, when considered in tandem with Tajima's D can be
368 prescriptive of specific evolutionary scenarios, such as purifying selection (low heterozygosity,
369 negative value of D) or a bottleneck (low heterozygosity and positive value of D), and gauges the
370 frequency of variants under the neutral model of evolution (Kimura 1968). The highest value for
371 nucleotide diversity across all BACs belongs to Australian *H. armigera* (0.018; in agreement with GBS
372 data), and is closely followed by the remainder of the *H. armigera* populations, the lowest of which
373 are of European origin (0.012). Generally, nucleotide diversity is higher among *H. armigera*
374 populations than in other species, though the highest seen in other species belongs jointly to *H. zea*
375 from Brazil, *H. assulta*, and *H. punctigera*, at 0.01 each, while the lowest is observed in *Heliothis*
376 *virescens* (Table S6). In respect of this, Tajima's D is generally positive for all populations of *H.*
377 *armigera*, except for Australian individuals. The only other instance whereby Tajima's D is negative is

378 apparent in *H. punctigera*, which is endemic to Australia. The highest Tajima's D values belong to
379 European *H. armigera* and *H. assulta*, at 0.32 and 0.47, respectively.

380 *Measurement of gene flow using the D statistic*

381 The highest level of *D* between *H. armigera* populations signifies gene flow between Australian and
382 New Zealand populations ($D = -0.204$) (Table 4). The next highest is between Australia and China ($D = -$
383 0.182). Brazilian populations present the lowest levels of gene flow ($D = -0.138$), and are followed by
384 individuals representing *H. armigera* from Senegal ($D = -0.149$). When focusing on gene flow into or
385 from Brazilian samples, *D* is highest for European samples ($D = -0.180$), with Senegalese *H. armigera*
386 found to have the next greatest level of gene flow ($D = -0.164$), whereas populations from Australia
387 and New Zealand have the lowest estimated levels ($D = -0.138$ and -0.143 , respectively). Gene flow
388 into *H. zea* from the USA is strongest from Brazilian *H. zea* ($D = 0.595$) and there is no evidence
389 demonstrating greater levels of gene flow between *H. armigera* from Brazil into Brazilian *H. zea*, over
390 *H. zea* from the USA.

391 *Selection across the CYP337B3 BAC*

392 Individuals genotyped for the haplotypes of the *CYP337B3* chimeric gene located on BAC 33J17
393 (JQ995292.1) formed clusters associated with the discrete selection events postulated to have
394 occurred in the development of resistance to fenvalerate (Fig. 8). For example, clusters reflecting
395 African, Asian and Australian origins for each of the haplotypes generally support geographical
396 origins of samples, with the first 2 principle components considered significant via Tracy-Widom
397 statistic ($P \leq 5.66 \times 10^{-21}$). This approach groups Brazilian samples with the Asian haplotype, while there
398 is evidence that certain samples that are distinguishable from the most populous clusters are in fact
399 heterozygotes, either in that they are heterozygous for the presence of the chimeric gene or are
400 heterozygous for specific *CYP337B3* haplotypes. This is supported by genotypes derived from Sanger

401 sequencing, which were able to bin samples under haplotypes described in Walsh et al. (Submitted)
402 (Table S7).

403 With regard to population genetic statistics across the BAC derived from clusters of individuals
404 identified in eigenstrat that corroborate with Sanger sequencing, we were able to compare the
405 evolutionary processes affecting genes associated with resistance to the pesticide fenvalerate (Fig.
406 9). On average, African samples had the most genetic diversity (0.026), in comparison to Asian
407 (0.022) and Australian individuals (0.018). Extremely low nucleotide diversity was found proximal to
408 the B3 gene (yellow bars in the figure legend), signifying selection at this site in all three populations.
409 Tajima's D is variable across the BAC, with an average of 0.92 for African individuals, 0.41 for Asian
410 and -0.46 for Australian populations. The lowest figure for Tajima's D was observed among Australian
411 individuals (-2.17, 81.25 kb), which is the approximate region in which the B3 exons lie. Though this
412 isn't apparent unless the size of the sliding windows is reduced to 1,250 bp (Fig. S4), Tajima's D is
413 highest (2.86) at the same location in African samples, as well as towards the end of the BAC
414 (Tajima's D= 2.04) and is likely the result of multiple alleles for this gene occurring in Africa.
415 Subsequently, the next highest Tajima's D value occurs at 88.75 kb in Australian samples, only a short
416 distance from B3. High Tajima's D in the region following from the B3 exons is likely the result of
417 relatively high levels of nucleotide diversity seen in all populations, though only Asian and African
418 populations see high nucleotide diversity preceding them.

419 Discussion

420 *Source of the Brazilian incursion*

421 Previous attempts have demonstrated that resolving population structure and gaining insight into
422 gene flow between populations of *H. armigera* is difficult, even at a continental scale. Here, we have
423 demonstrated that high-throughput sequencing methods are capable of resolving genetic variation
424 associated with specific geographic localities. Specifically, we show that European *H. armigera* are

425 most similar to Brazilian samples and we are unable to see a pattern in individuals collected in Africa
426 and Asia. The first molecular identification of *H. armigera* in Brazil suggested that, even from a
427 limited collection, samples were likely derived from a number of maternal lineages that are prevalent
428 throughout the Old World (Tay *et al.* 2013). Subsequent work identified the distribution of variation
429 at the B3 allele, which contributes towards fenvalerate resistance (Walsh *et al.* submitted),
430 represented regional dominance of specific variants that were likely independently generated
431 throughout Australasia, Africa and Asia. Of these, alleles found most frequently in Asia were seen in
432 both African and Australian populations, but dominated those documented in Brazil, which also bore
433 a single African allele.

434 We find that our data broadly agree with previous findings; variation across the BAC containing the
435 *CYP337B3* gene demonstrates that all *H. armigera* sampled in Brazil bear the variant considered to
436 have originated in Asian populations, with other individuals broadly sorted into the most prevalent
437 geographic variants observed by Walsh *et al.* (submitted). While populations remain poorly resolved
438 when considering variants mapped across other BACs, sophisticated analytical techniques have
439 demonstrated that the greatest levels of gene flow occur between European and Brazilian *H.*
440 *armigera*. Individuals sampled from Europe were also found to possess *CYP337B3* alleles most
441 commonly found in Asia and Africa, likely the result of high degrees of admixture from these regions.
442 This is spatially intuitive given that one would expect African and Asian populations to mix in this
443 region and that the west coast of Africa, is the closest continental landmass to Brazil. The latter point
444 is validated through the levels of gene flow inferred between Brazilian and Senegalese *H. armigera*
445 (outputting the second highest value of *D* in these analyses). Showing that the incursion is likely
446 sourced from a diverse population, has important implications in that the invasive population will
447 possess greater genetic variation that will increase adaptive potential (Lavergne & Molofsky 2007).
448 This is supported with levels of nucleotide diversity in the Brazilian individuals that are similar to
449 other populations in both high-throughput data sets. We also see the highest levels of inbreeding

450 coefficient, which, in tandem with high nucleotide diversity is synonymous with an incursion by a
451 diverse population (Blackburn *et al.* 2015).

452 *Population structure in H. armigera*

453 Within our analyses, we are clearly able to distinguish two discrete populations of *H. armigera*. This
454 reflects a distinction between *H. armigera armigera* and *H. armigera conferta* as has been previously
455 identified by taxonomists (Hardwick 1965; Matthews 1999). *H. armigera conferta* has been
456 considered to be restricted to Australasia, with individuals being distinguishable from the rest of the
457 global *H. armigera* population in our analyses. Australian populations share the most genetic
458 variation with individuals from New Zealand, and to a lesser extent, China. Notably, a single Chinese
459 individual shares a large degree of genetic variation with Australian *H. armigera*. The distinction
460 between subspecies is not as extreme in individuals from New Zealand and implies that gene flow
461 from China to New Zealand is stronger than that into Australia. This may suggest differences in issues
462 effecting biosecurity or perhaps that Australian populations are less susceptible to invasion. Tajima's
463 *D* across BACs belonging to *H. armigera* from New Zealand is at a similar level to other well-
464 established *H. armigera* populations, but is only negative in Australian individuals and *H. punctigera*
465 and might highlight Australia-specific evolutionary processes that could be imposed by region-
466 specific climactic events or agricultural practices. Analogous results are seen in an attempt to identify
467 gene flow between populations of *H. armigera*, made by Song *et al.* (2015) who analysed 9 sex
468 chromosome-linked EPIC markers, which use primers in adjacent exons to span intronic sequences.
469 These authors found little population structure among geographic regions similar to those assessed
470 in our study but at one locus in particular, they identified a distinction between Australian *H.*
471 *armigera* and those from Africa and Asia and suggested that there is likely a significant degree of
472 gene flow between Australian and Chinese populations. The fact that we see a Chinese individual
473 bearing a greater resemblance to Australian *H. armigera* suggests that the distinction between *H.*

474 *armigera armigera* and *H. armigera conferta* may act as a potential model for hybridisation between
475 Heliothine species in the New World. Primarily, the comparison offers an example of what can be
476 expected when two genetically distinct populations from differing climates, subject to alternative
477 agricultural practices and pest management, come into contact. Admixture between subspecies in
478 the Asia-Pacific region could provide insight into the spread of resistance genes, the biosecurity
479 measures that are able to restrict movement, and what evolutionary patterns may be expected in
480 the New World. At the very least, through our data, we recognise gene flow between these regions
481 and acknowledge that biosecurity would gain insight as to movements across this region with
482 continued genotyping efforts.

483 While we are unable to resolve meaningful population structure between China, India and Uganda
484 across GBS or whole-genome sequences, they remain relatively distinguishable from Brazilian
485 populations, with particular insight demonstrable in the large number of private alleles and in
486 patterns of missing genotypes observed in the GBS data. Missing data in GBS may be caused by an
487 interruption of the recognition site of restriction enzymes, biases introduced during library
488 preparation, sequencing biases, or inadequate coverage. While we feel it would be inappropriate to
489 comment upon population structure using this missing data at this time, there may be signals of
490 variation associated with specific geographic regions when the whole genome is analysed.

491 Interactions between populations of *H. armigera* over large spatial ranges as we've demonstrated
492 are unsurprising. Many noctuid moths are, in fact, facultative migrants that are capable of using wind
493 flow to take flight in response to environmental conditions (Bowden & Johnson 1976; Nibouche *et al.*
494 1998; Jones *et al.* 2015). Recent experiments using *H. armigera* have recorded that individuals are
495 capable of flying between 20 and 40 km in a single night using tethered laboratory simulations (Jones
496 *et al.* 2015). Within the mitochondrial genome tree presented here, we can see that *H. gelotopoeon*,
497 found only in South America, shares a common ancestor with *H. punctigera*, whose distribution is

498 restricted exclusively to Australia (Fitt 1989), thus insinuating the spread of noctuides across the
499 Pacific Ocean, previously. Though a number of insect species are capable of similar feats of extensive
500 migratory flight, many are unable to maintain population density in South America. This includes the
501 Painted lady, *Vanessa cardui*, and the locust, *Locusta migratoria* (Rosenberg & Burt; Stefanescu *et al.*
502 2013), while a single incursion of the desert locust, *Schistocerca gregaria*, is likely the source of
503 several contemporary species now found in the New World (Lovejoy *et al.* 2006). In an example most
504 pertinent to the spread of *H. armigera* into the New World, monarch butterflies (*Danaus plexippus*),
505 have dispersed across the Atlantic and Pacific oceans, as demonstrated by Zhan *et al.* (2014). These
506 authors used whole genome sequencing of individuals from a number of populations along the
507 species distribution to elaborate upon demographic history and were able to highlight candidate
508 genes associated with migration and colour morphology. While the intercontinental spread of
509 migratory species has been documented in several instances, it remains difficult to distinguish the
510 natural spread from an anthropogenic cause, though geographic distances will play a great role in the
511 interpretation. Further work using archived *H. armigera*, caught early on in the incursion, might
512 therefore be useful for identifying not only the source of the incursion. This would perhaps define
513 the basis for migratory performance while simultaneously defining the role of humans in the spread
514 of *H. armigera* into the New World.

515 *Hybridisation between H. armigera and H. zea*

516 The single, clearest distinction that we're able to make throughout these analyses is that between *H.*
517 *armigera* and *H. zea*, though this may become more difficult if *H. armigera* is able to successfully
518 spread and hybridise throughout the New World. Even the clearly observable distinction made via
519 mitochondrial markers may, in time, represent a series of haplogroups or be lost entirely, as is
520 observable in modern humans, who show genomic evidence for admixture with Neanderthals
521 though no mitochondrial haplogroups exist (Ghirotto *et al.* 2011; Sankararaman *et al.* 2012). It is

522 possible that *H. zea* has facilitated the arrival of *H. armigera* into the New World, as we have
523 presented putative evidence of a naturally occurring hybrid within our GBS data, which is
524 characterised as having mitochondrial DNA originating from *H. zea*, but shares a considerable
525 proportion of genomic DNA between genotypes clustering with both *H. armigera* and *H. zea*. Similar
526 patterns were used recently to distinguish naturally occurring hybrids between golden jackals (*Canis*
527 *aureus*) and domestic dogs (*Canis familiaris*) (Galov *et al.* 2015). The use of laboratory crosses to
528 confirm patterns of heredity in the Galov *et al.* (2015) study greatly supported the author's
529 inferences and as such, understanding the capability of *H. armigera* and *H. zea* to hybridise across
530 multiple generations cannot be understated and should serve as a principle goal for future research.

531 Sequencing the genomes of these two species will provide not only an insight into the relative
532 ancestry of individuals in the future, but will allow for interpretation of what makes *H. armigera* such
533 a successful pest. Genomic analyses will also identify additional regions of the genome that are likely
534 to be under selection among emerging populations of *H. armigera* and this will have implications as
535 to the magnitude of the species as a pest in the New World. For example, using a range of methods
536 that make use of high-throughput sequencing, it is possible to estimate the extent of linkage
537 disequilibrium across the genome and estimate the likelihood of introgression with species-specific
538 haplotypes as in works analysing humans and Neanderthals (Sankararaman *et al.* 2012, 2014).

539 Therefore, the *H. armigera/H. zea* model has the potential to act, not only as an exemplary
540 evolutionary model for incursive and introgressive processes, but also as an important indicator of
541 susceptibility in global biosecurity. Indeed, recent work in monarch butterflies made use of whole-
542 genome sequencing combined with phenotypes to provide insights into migratory behaviour and
543 morphology (Zhan *et al.* 2014). A similar approach would improve the power of such analyses in pest
544 species, although gaining phenotypic data relevant to resistance across a global sampling effort
545 remains a logistical problem. Through the use of whole-genome sequencing, and based upon a
546 wealth of previous work into the bases of resistance, we've been able to show that tight regions

547 around the *CYP337B3* gene are under selection in all of the haplogroups assessed. This likely reflects
548 that the populations are under selection and represents the value of monitoring populations so as to
549 infer evolutionary processes. For example, if the population has recently undergone a bottleneck,
550 then the impact of measures to control for pesticide resistance might have longer lasting effects if
551 implemented in this population rather than a population undergoing purifying selection. Genes
552 associated with resistance to pesticides play a definitive role in monitoring gene flow, are the most
553 relevant for managing agricultural practices, and will play a key role in observing interactions
554 between *H. armigera* and *H. zea* in the New World.

555 **Conclusion**

556 For the majority of *H. armigera* populations assessed, population structure remains unclear following
557 interrogation with a number of analyses based upon high-throughput sequencing. Though we were
558 unable to resolve populations with more than 12 kb of the mitochondrial genome, we are able to
559 make a number of distinctions that are clearly important to the future of research in this area.
560 Primarily, we are able to suggest that Brazilian *H. armigera* likely originated from Europe or West
561 Africa, based upon whole genome sequences aligned to BACs. Using the same data, we were able to
562 distinguish a subspecies of *H. armigera* generally endemic to Australasia and distinct from other
563 populations. This inference was discernible in *de novo* GBS data, and was also apparent when a gene
564 associated with resistance to fenvalerate was examined. Further analyses demonstrated that this
565 gene is likely under selection and supports the perspective that agriculturally relevant genes can be
566 used to not only monitor the spread of resistance but also to differentiate populations. Importantly,
567 we highlight a potential example of natural hybridisation between *H. armigera* and *H. zea*, which sets
568 a strong precedent for future research in establishing the capability of these species to hybridise. The
569 end points presented here supply a series of provocative insights into the recent evolutionary history

570 of a destructive pest species, but superior insight will only become apparent as genomic resources
571 for these species become available.

572 **Acknowledgments**

573 We thank Andreas Zwick for providing the *Helicoverpa hardwickii* for these analyses. This work was
574 funded under the CSIRO OCE postdoctoral scheme.

575 **Author Contributions**

576 CA and TKW wrote the manuscript. WTT and TKW organised sample collection. CA, WTT and TKW
577 prepared DNA, made libraries and analysed the data. All authors provided intellectual input and
578 contributed to organising the work. All authors edited the manuscript and endorse its submission.

579 **References**

- 580 Allendorf FW, Hohenlohe PA, Luikart G (2010) Genomics and the future of conservation genetics.
581 *Nature reviews. Genetics*, **11**, 697–709.
- 582 Altschul SF, Gish W, Miller W, Myers EW, Lipman DJ (1990) Basic local alignment search tool. *Journal*
583 *of molecular biology*, **215**, 403–10.
- 584 Andrews KR, Good JM, Miller MR, Luikart G, Hohenlohe PA (2016) Harnessing the power of RADseq
585 for ecological and evolutionary genomics. *Nature Reviews Genetics*, **17**, 81–92.
- 586 Behere GT, Tay WT, Russell D a *et al.* (2007) Mitochondrial DNA analysis of field populations of
587 *Helicoverpa armigera* (Lepidoptera: Noctuidae) and of its relationship to *H. zea*. *BMC*
588 *evolutionary biology*, **7**, 117.
- 589 Behere GT, Tay WT, Russell DA, Kranthi KR, Batterham P (2013) Population genetic structure of the
590 cotton bollworm *Helicoverpa armigera* (Hübner) (Lepidoptera: Noctuidae) in India as inferred
591 from EPIC-PCR DNA markers. *PLoS one*, **8**, e53448.
- 592 Blackburn TM, Lockwood JL, Cassey P (2015) The influence of numbers on invasion success.
593 *Molecular ecology*, **24**, 1942–53.
- 594 Bowden J, Johnson CG (1976) Migrating and other terrestrial insects at sea. In: *Marine Insects* (ed
595 Cheng L), pp. 97–118. North-Holland Publishing Company, Oxford.

- 596 Catchen J, Bassham S, Wilson T *et al.* (2013a) The population structure and recent colonization
597 history of Oregon threespine stickleback determined using restriction-site associated DNA-
598 sequencing. *Molecular ecology*, **22**, 2864–83.
- 599 Catchen J, Hohenlohe PA, Bassham S, Amores A, Cresko WA (2013b) Stacks: an analysis tool set for
600 population genomics. *Molecular ecology*, **22**, 3124–40.
- 601 Chevreux B, Pfisterer T, Drescher B *et al.* (2004) Using the miraEST assembler for reliable and
602 automated mRNA transcript assembly and SNP detection in sequenced ESTs. *Genome research*,
603 **14**, 1147–59.
- 604 Cho S, Mitchel A, Mitter C *et al.* (2008) Molecular phylogenetics of heliothine moths (Lepidoptera:
605 Noctuidae: Heliiothinae), with comments on the evolution of host range and pest status.
606 *Systematic Entomology*, **33**, 581–594.
- 607 Czepak C, Albernaz KC, Vivian LM, Guimarães HO, Carvalhais T (2013) First reported occurrence of
608 *Helicoverpa armigera* (Hubner) (Lepidoptera: Noctuidae) in Brazil. *Pesquisa Agropecuaria*
609 *Tropical*, **43**, 110–113.
- 610 Danecek P, Auton A, Abecasis G *et al.* (2011) The variant call format and VCFtools. *Bioinformatics*
611 (Oxford, England), **27**, 2156–8.
- 612 Davey JW, Hohenlohe PA, Etter PD *et al.* (2011) Genome-wide genetic marker discovery and
613 genotyping using next-generation sequencing. *Nature reviews. Genetics*, **12**, 499–510.
- 614 Durand EY, Patterson N, Reich D, Slatkin M (2011) Testing for Ancient Admixture between Closely
615 Related Populations. *Molecular Biology and Evolution*, **28**, 2239–2252.
- 616 Earl D a., vonHoldt BM (2012) STRUCTURE HARVESTER: a website and program for visualizing
617 STRUCTURE output and implementing the Evanno method. *Conservation Genetics Resources*, **4**,
618 359–361.
- 619 Evanno G, Regnaut S, Goudet J (2005) Detecting the number of clusters of individuals using the
620 software STRUCTURE: a simulation study. *Molecular ecology*, **14**, 2611–20.
- 621 Excoffier L, Smouse PE, Quattro JM (1992) Analysis of molecular variance inferred from metric
622 distances among DNA haplotypes: Application to human mitochondrial DNA restriction data.
623 *Genetics*, **131**, 479–491.
- 624 Falush D, Stephens M, Pritchard JK (2007) Inference of population structure using multilocus
625 genotype data: dominant markers and null alleles. *Molecular ecology notes*, **7**, 574–578.
- 626 Feng HQ, Wu KM, Ni YX, Cheng DF, Guo YY (2005) High-altitude windborne transport of *Helicoverpa*
627 *armigera* (Lepidoptera : Noctuidae) in mid-summer in northern China. *Journal of Insect*
628 *Behavior*, **18**, 335–349.
- 629 Fitt GP (1989) The Ecology of *Heliothis* Species in Relation to Agroecosystems. *Annual Reviews*
630 *Entomology*, **34**, 17–52.

- 631 Forster P, Ro A (1994) Median-Joining Networks for Inferring Intraspecific Phylogenies. *Molecular*
632 *Biology and Evolution*, **16**, 37–48.
- 633 Galov A, Fabbri E, Caniglia R *et al.* (2015) First evidence of hybridization between golden jackal (*Canis*
634 *aureus*) and domestic dog (*Canis familiaris*) as revealed by genetic markers. *Royal Society*
635 *Open Science*, **2**, 150450.
- 636 Ghirotto S, Tassi F, Benazzo A, Barbujani G (2011) No evidence of Neandertal admixture in the
637 mitochondrial genomes of early European modern humans and contemporary Europeans.
638 *American journal of physical anthropology*, **146**, 242–52.
- 639 Gunning R V, Dang HT, Kemp FC, Nicholson IC, Moores GD (2005) New resistance mechanism in
640 *Helicoverpa armigera* threatens transgenic crops expressing *Bacillus thuringiensis* Cry1Ac toxin.
641 *Applied and environmental microbiology*, **71**, 2558–63.
- 642 Hahn C, Bachmann L, Chevreaux B (2013) Reconstructing mitochondrial genomes directly from
643 genomic next-generation sequencing reads—a baiting and iterative mapping approach. *Nucleic*
644 *acids research*, **41**, e129.
- 645 Hardwick DF (1965) The Corn Earworm Complex. *Memoirs of the Entomological Society of Canada*,
646 **97**, 1–247.
- 647 Hayden J, Brambila J (2015) *Florida Department of Agriculture and Consumer Services Division of*
648 *Plant Industry*.
- 649 Jin L, Zhang H, Lu Y *et al.* (2015) Large-scale test of the natural refuge strategy for delaying insect
650 resistance to transgenic Bt crops. *Nature biotechnology*, **33**, 169–74.
- 651 Jones CM, Papanicolaou A, Mironidis GK *et al.* (2015) Genomewide transcriptional signatures of
652 migratory flight activity in a globally invasive insect pest. *Molecular ecology*, **24**, 4901–11.
- 653 Joußen N, Agnolet S, Lorenz S *et al.* (2012) Resistance of Australian *Helicoverpa armigera* to
654 fenvalerate is due to the chimeric P450 enzyme CYP337B3. *Proceedings of the National*
655 *Academy of Sciences of the United States of America*, **109**, 15206–11.
- 656 Kalinowski ST (2004) Counting Alleles with Rarefaction: Private Alleles and Hierarchical Sampling
657 Designs. *Conservation Genetics*, **5**, 539–543.
- 658 Katoh K (2002) MAFFT: a novel method for rapid multiple sequence alignment based on fast Fourier
659 transform. *Nucleic Acids Research*, **30**, 3059–3066.
- 660 Kimura M (1968) Evolutionary Rate at the Molecular Level. *Nature*, **217**, 624–626.
- 661 Kirk H, Dorn S, Mazzi D (2013) Molecular genetics and genomics generate new insights into
662 invertebrate pest invasions. *Evolutionary Applications*, **6**, 842–856.
- 663 Kriticos DJ, Ota N, Hutchison WD *et al.* (2015) The potential distribution of invading *Helicoverpa*
664 *armigera* in North America: is it just a matter of time? *PLoS one*, **10**, e0119618.

- 665 Laster ML, Hardee DD (1995) Interbreeding Compatibility Between North American *Helicoverpa zea*
666 and *Heliothis armigera* (Lepidoptera: Noctuidae) from Russia. *Journal of Economic Entomology*,
667 **88**, 77–80.
- 668 Laster M, Sheng C (1995) Search for Hybrid Sterility for *Helicoverpa-Zea* in Crosses between the
669 North-American *Heliothis-Zea* and *Helicoverpa-Armigera* (Lepidoptera, Noctuidae) from China.
670 *Journal of Economic Entomology*, **88**, 1288–1291.
- 671 Lavergne S, Molofsky J (2007) Increased genetic variation and evolutionary potential drive the
672 success of an invasive grass. *Proceedings of the National Academy of Sciences of the United*
673 *States of America*, **104**, 3883–8.
- 674 Leigh JW, Bryant D (2015) popart : full-feature software for haplotype network construction (S
675 Nakagawa, Ed.). *Methods in Ecology and Evolution*, **6**, 1110–1116.
- 676 Li H, Handsaker B, Wysoker A *et al.* (2009) The Sequence Alignment/Map format and SAMtools.
677 *Bioinformatics (Oxford, England)*, **25**, 2078–9.
- 678 Lovejoy NR, Mullen SP, Sword GA, Chapman RF, Harrison RG (2006) Ancient trans-Atlantic flight
679 explains locust biogeography: molecular phylogenetics of *Schistocerca*. *Proceedings. Biological*
680 *sciences / The Royal Society*, **273**, 767–74.
- 681 Malinsky M, Challis RJ, Tyers AM *et al.* (2015) Genomic islands of speciation separate cichlid
682 ecomorphs in an East African crater lake. *Science*, **350**, 1493–1498.
- 683 Martin SH, Dasmahapatra KK, Nadeau NJ *et al.* (2013) Genome-wide evidence for speciation with
684 gene flow in *Heliconius* butterflies. *Genome research*, **23**, 1817–28.
- 685 Matthews M (1999) *Heliothine moths of Australia. A guide to pest bollworms and related noctuid*
686 *groups*. CSIRO Publishing, Collingwood, Australia.
- 687 McCaffery AR (1998) Resistance to insecticides in Heliothine Lepidoptera: a global view. *Philosophical*
688 *Transactions of the Royal Society B: Biological Sciences*, **353**, 1735–1750.
- 689 McKenna A, Hanna M, Banks E *et al.* (2010) The Genome Analysis Toolkit: a MapReduce framework
690 for analyzing next-generation DNA sequencing data. *Genome research*, **20**, 1297–303.
- 691 Nadachowska-Brzyska K, Burri R, Olason PI *et al.* (2013) Demographic divergence history of pied
692 flycatcher and collared flycatcher inferred from whole-genome re-sequencing data. *PLoS*
693 *genetics*, **9**, e1003942.
- 694 Nibouche S, Buès R, Toubon J-F, Poitout S (1998) Allozyme polymorphism in the cotton bollworm
695 *Helicoverpa armigera* (Lepidoptera: Noctuidae): comparison of African and European
696 populations. *Heredity*, **80**, 438–445.
- 697 Patterson N, Moorjani P, Luo Y *et al.* (2012) Ancient admixture in human history. *Genetics*, **192**,
698 1065–93.
- 699 Patterson N, Price AL, Reich D (2006) Population structure and eigenanalysis. *PLoS genetics*, **2**, e190.

- 700 Posada D (2008) jModelTest: phylogenetic model averaging. *Molecular biology and evolution*, **25**,
701 1253–6.
- 702 Prado-Martinez J, Sudmant PH, Kidd JM *et al.* (2013) Great ape genetic diversity and population
703 history. *Nature*, **499**, 471–5.
- 704 Pritchard JK, Stephens M, Donnelly P (2000) Inference of population structure using multilocus
705 genotype data. *Genetics*, **155**, 945–59.
- 706 Purcell S, Neale B, Todd-Brown K *et al.* (2007) PLINK: a tool set for whole-genome association and
707 population-based linkage analyses. *American journal of human genetics*, **81**, 559–75.
- 708 R Core Team (2014) *R: a language and environment for statistical computing*. R Foundation for
709 Statistical Computing, Vienna, Austria.
- 710 Rasool A, Joußen N, Lorenz S *et al.* (2014) An independent occurrence of the chimeric P450 enzyme
711 CYP337B3 of *Helicoverpa armigera* confers cypermethrin resistance in Pakistan. *Insect*
712 *biochemistry and molecular biology*, **53**, 54–65.
- 713 Ronquist F, Huelsenbeck JP (2003) MrBayes 3: Bayesian phylogenetic inference under mixed models.
714 *Bioinformatics*, **19**, 1572–1574.
- 715 Rosenberg J, Burt PJA Windborne displacements of Desert Locusts from Africa to the Caribbean and
716 South America. *Aerobiologia*, **15**, 167–175.
- 717 Sankararaman S, Mallick S, Dannemann M *et al.* (2014) The genomic landscape of Neanderthal
718 ancestry in present-day humans. *Nature*, **507**, 354–7.
- 719 Sankararaman S, Patterson N, Li H, Pääbo S, Reich D (2012) The date of interbreeding between
720 Neandertals and modern humans. *PLoS genetics*, **8**, e1002947.
- 721 Song S V, Downes S, Parker T, Oakeshott JG, Robin C (2015) High nucleotide diversity and limited
722 linkage disequilibrium in *Helicoverpa armigera* facilitates the detection of a selective sweep.
723 *Heredity*, **115**, 460–70.
- 724 Sousa V, Hey J (2013) Understanding the origin of species with genome-scale data: modelling gene
725 flow. *Nature reviews. Genetics*, **14**, 404–14.
- 726 Stefanescu C, Páramo F, Åkesson S *et al.* (2013) Multi-generational long-distance migration of insects:
727 studying the painted lady butterfly in the Western Palaearctic. *Ecography*, **36**, 474–486.
- 728 Talavera G, Castresana J (2007) Improvement of phylogenies after removing divergent and
729 ambiguously aligned blocks from protein sequence alignments. *Systematic biology*, **56**, 564–77.
- 730 Tamura K, Stecher G, Peterson D, Filipski A, Kumar S (2013) MEGA6: Molecular Evolutionary Genetics
731 Analysis version 6.0. *Molecular biology and evolution*, **30**, 2725–9.

- 732 Tay WT, Mahon RJ, Heckel DG *et al.* (2015) Insect Resistance to *Bacillus thuringiensis* Toxin Cry2Ab Is
733 Conferred by Mutations in an ABC Transporter Subfamily A Protein. *PLoS genetics*, **11**,
734 e1005534.
- 735 Tay WT, Soria MF, Walsh T *et al.* (2013) A brave new world for an old world pest: *Helicoverpa*
736 *armigera* (Lepidoptera: Noctuidae) in Brazil. *PLoS ONE*, **8**, e80134.
- 737 Veeramah KR, Hammer MF (2014) The impact of whole-genome sequencing on the reconstruction of
738 human population history. *Nature reviews. Genetics*, **15**, 149–62.
- 739 Walsh T, Joußen N, Tian K *et al.* Multiple recombination events between two cytochrome P450 loci
740 contribute to global pyrethroid resistance in *Helicoverpa armigera*. *Submitted*.
- 741 Wickham H (2009) *ggplot2*. Springer New York, New York, NY.
- 742 Yang Y, Li Y, Wu Y (2013) Current Status of Insecticide Resistance in *Helicoverpa armigera*
743 After 15 Years of Bt Cotton Planting in China. *Journal of Economic Entomology*, **106**, 375–381.
- 744 Zhan S, Zhang W, Niitepöld K *et al.* (2014) The genetics of monarch butterfly migration and warning
745 colouration. *Nature*, **514**, 317–21.

746

747 **Data Accessibility**

748 Alignment of mtDNA genomes: Dryad entry XXX

749 VCF of B3 BAC alignments: Dryad entry XXX

750 Plink format data for the GBS data: Dryad entry XXX

751

752

753

754

755

756 **Tables**

757 Table 1. Summary genetic statistics at variant positions in populations of *H. armigera* and *H. zea*
 758 assessed using GBS, including nucleotide diversity (π) and Wright's inbreeding coefficient (*Fis*).

Population	Private Alleles	Observed Heterozygosity	π	<i>Fis</i>
Australia	339	0.027	0.029	0.009
China	243	0.025	0.028	0.011
India	253	0.024	0.029	0.019
Uganda	318	0.024	0.028	0.020
Brazil	767	0.019	0.027	0.068
USA zea	88	0.015	0.015	0.002
Brazil zea	120	0.017	0.016	-0.001
Brazil zea 2	122	0.013	0.016	0.012

759

760

761 Table 2. Evidence for gene flow between populations of heliothine moth determined from GBS data.
 762 Significant calculations of *D* are in bold.

<i>D</i> (<i>H. punctigera</i> , <i>x</i> ; <i>y</i> , <i>H. zea</i> (USA))			
Population <i>x</i>	Population <i>y</i>	<i>D</i>	Z-score
Australia	China	-0.259	-3.88
Australia	Brazil	-0.198	-2.75
Australia	Uganda	-0.198	-2.78
Australia	India	-0.196	-2.90
Australia	Brazil zea	0.023	0.48
Australia	Brazil zea 2	0.078	2.22
China	Brazil	-0.270	-3.74
Uganda	Brazil	-0.259	-3.95
India	Brazil	-0.251	-3.44
Australia	Brazil	-0.198	-2.75
Brazil zea 2	Brazil	0.846	42.34
Brazil zea	Brazil	0.852	41.14
China	India	-0.262	-3.88
China	Uganda	-0.237	-3.31
India	Uganda	-0.206	-2.82
Brazil	Brazil zea	0.004	0.08

763

764 Table 3. Summary genetic statistics, including nucleotide diversity (π), for populations of *H. armigera*
 765 assessed using whole genome sequencing data aligned to all BACs.

Population	Tajima's <i>D</i>	π	Number of Samples
Australia	-0.370	0.018	17
Brazil	0.020	0.016	5
China	0.140	0.014	4
Europe	0.320	0.012	4
India	0.030	0.017	5
Madagascar	0.230	0.014	3
New Zealand	0.280	0.016	3
Senegal	0.190	0.016	3
Uganda	0.170	0.015	4

766

767 Table 4. Evidence for gene flow between populations of Heliothine moth determined from whole-
 768 genome sequences aligned to BACs. Significant calculations of *D* are in bold.

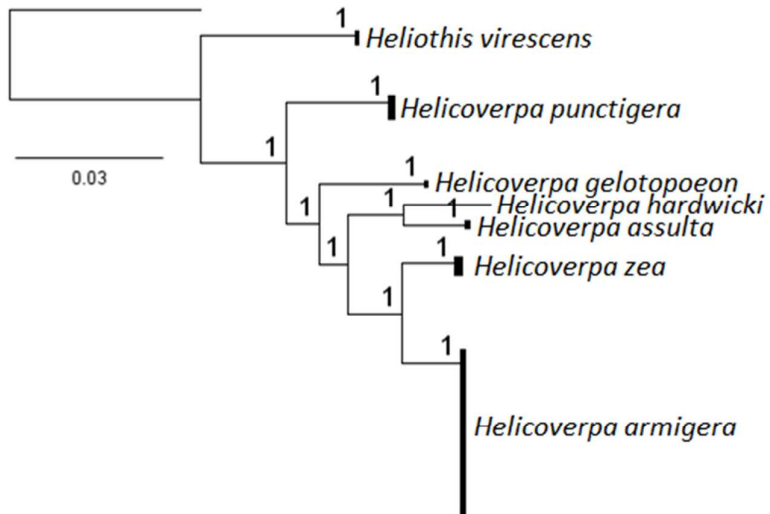
<i>D</i> (<i>H. Assulta</i> , <i>x</i> ; <i>y</i> , <i>H. zea</i> (USA))			
Population <i>x</i>	Population <i>y</i>	<i>D</i>	Z-score
New Zealand	Australia	-0.204	-9.45
China	Australia	-0.182	-9.32
Uganda	Australia	-0.172	-12.81
Europe	Australia	-0.171	-11.13
Madagascar	Australia	-0.158	-12.04
India	Australia	-0.156	-6.98
Senegal	Australia	-0.149	-10.63
Brazil	Australia	-0.138	-9.67
Brazil zea	Australia	0.595	28.81
Brazil	Europe	-0.180	-10.37
Brazil	Senegal	-0.164	-11.86
Brazil	China	-0.163	-11.09
Brazil	Uganda	-0.160	-9.55
Brazil	India	-0.155	-9.49
Brazil	Madagascar	-0.149	-10.33
Brazil	New Zealand	-0.143	-9.27
Brazil	Australia	-0.138	-9.67
Brazil	Brazil zea	0.007	0.64

769

770

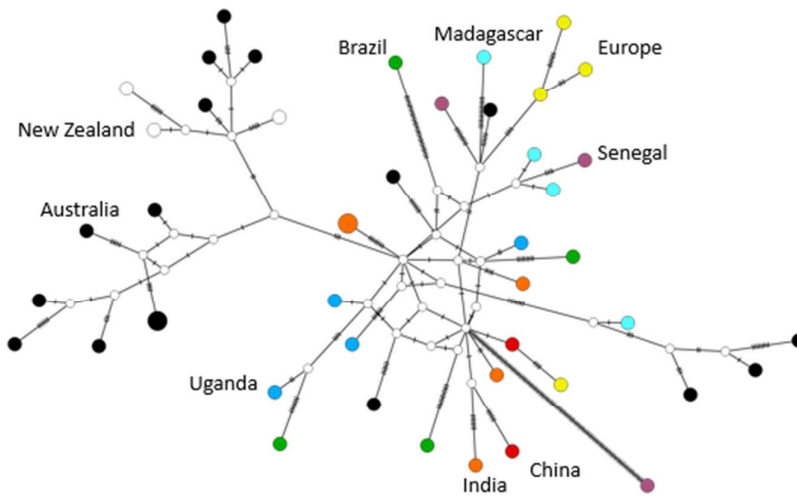
771 **Figures**

772 Fig. 1. Bayesian phylogenetic tree derived from 12,248 bp of the mitochondrial genome, showing the
 773 relationship of *H. armigera* with other heliothine species. Bootstrap values are shown above nodes
 774 and subtrees beyond species distinction have been contracted for clarity. *Spodoptera frugiperda* is
 775 the out group.



776

777 Fig. 2. Mitochondrial haplotype network of *H. armigera* from populations around the world. Hatch
 778 marks symbolise missing haplotypes and small, open circles represent hypothetical intermediates.



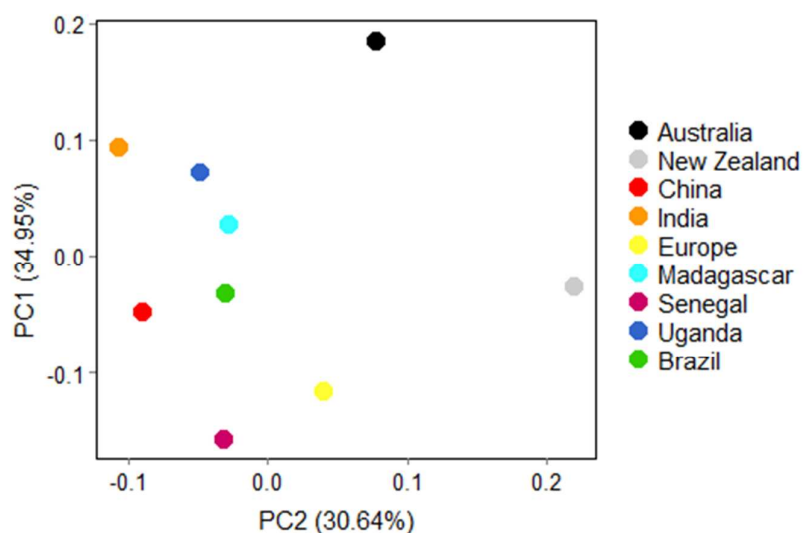
779

780

781

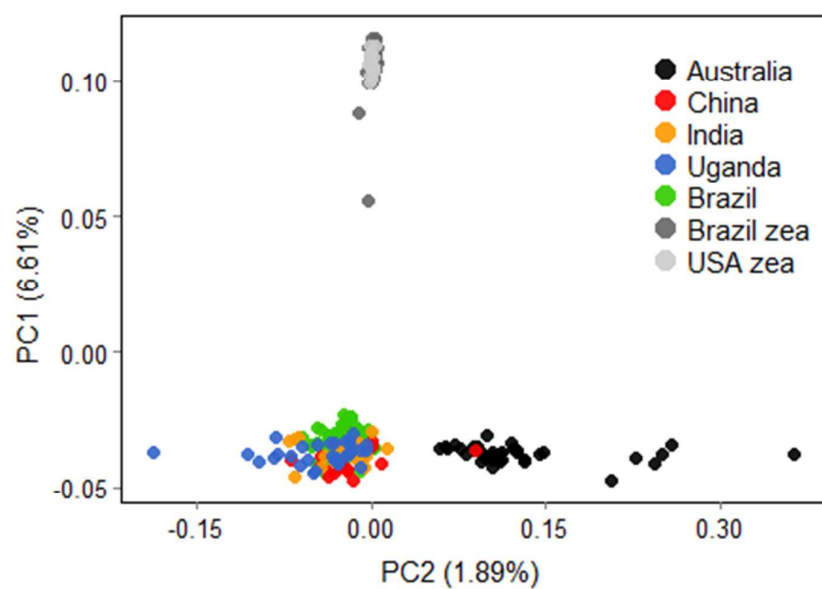
782

783 Fig. 3. Principle component analysis of Φ_{st} derived from mitochondrial variation in *H. armigera*
 784 populations. The amount of variance explained by each component is noted on their respective axes.



785

786 Fig. 4. Principle component analysis of GBS data for populations of *H. armigera* ($n=217$) and *H. zea*
 787 ($n=62$). The amount of variance explained by each component is noted on their respective axes.



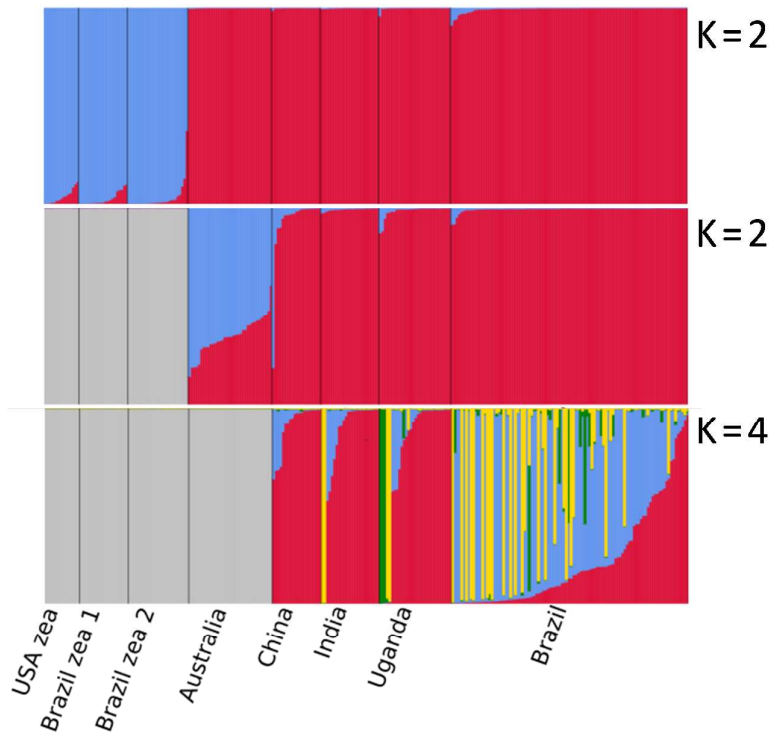
788

789

790

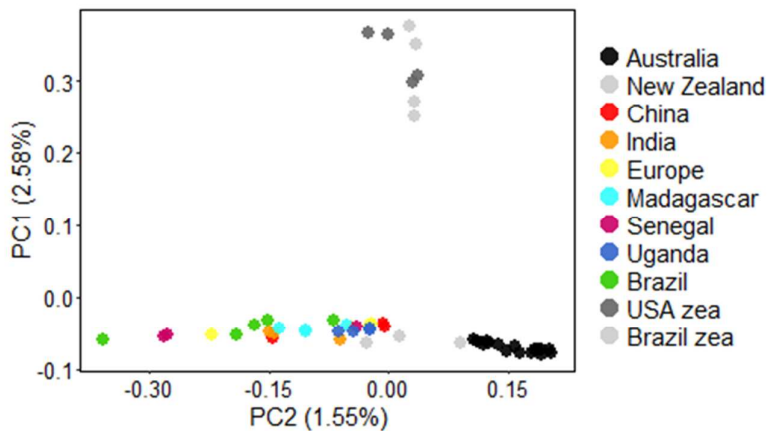
791

792 Fig. 5. Structure results from GBS data for *H. armigera* ($n=217$) and *H. zea* ($n=62$), highlighting the
 793 distinctions between *H. armigera* and *H. zea* (top), *H. armigera armigera* and *H. armigera conferta*
 794 (middle) and populations of *H. armigera armigera* (bottom). The grey colour reflects samples not
 795 used in the analysis and values of K found best to fit the data are next to their respective analyses.



796

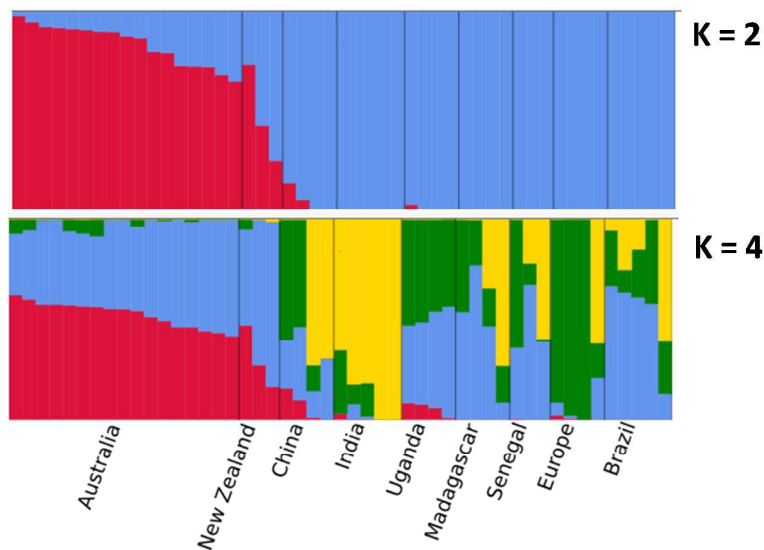
797 Fig. 6. Principle component analysis of *H. armigera* ($n=50$) and *H. zea* ($n=8$) variants derived from
 798 whole-genome sequences aligned to BACs. The amount of variance explained by each component is
 799 noted on their respective axes.



800

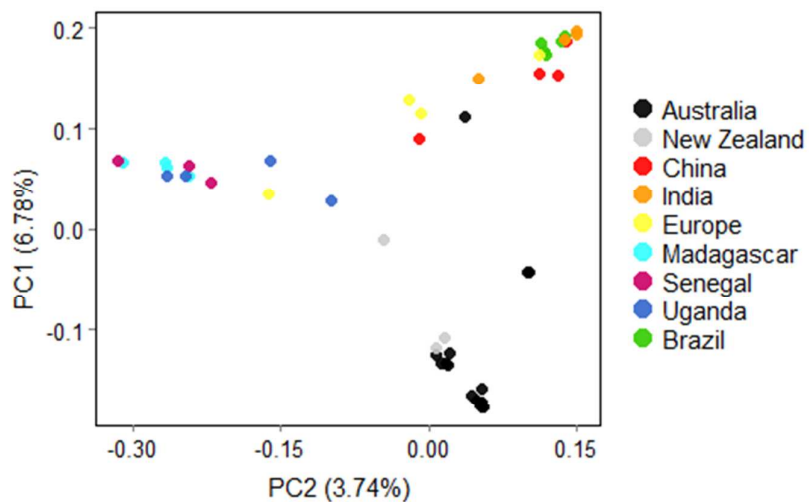
801

802 Fig. 7. Structure results derived from whole-genome sequences aligned to BACs, highlighting the
 803 distinctions between *H. armigera armigera* and *H. armigera conferta* (top) and populations of *H.*
 804 *armigera armigera* (bottom). Values of K found best to fit the data are next to their respective
 805 analyses.



806

807 Fig. 8. Principle component analysis of *H. armigera* sequencing data aligned to the 33J17 BAC
 808 (JQ995292.1) containing the CYP337B3 gene implicated in pyrethroid resistance. The amount of
 809 variance explained by each component is noted on their respective axes.



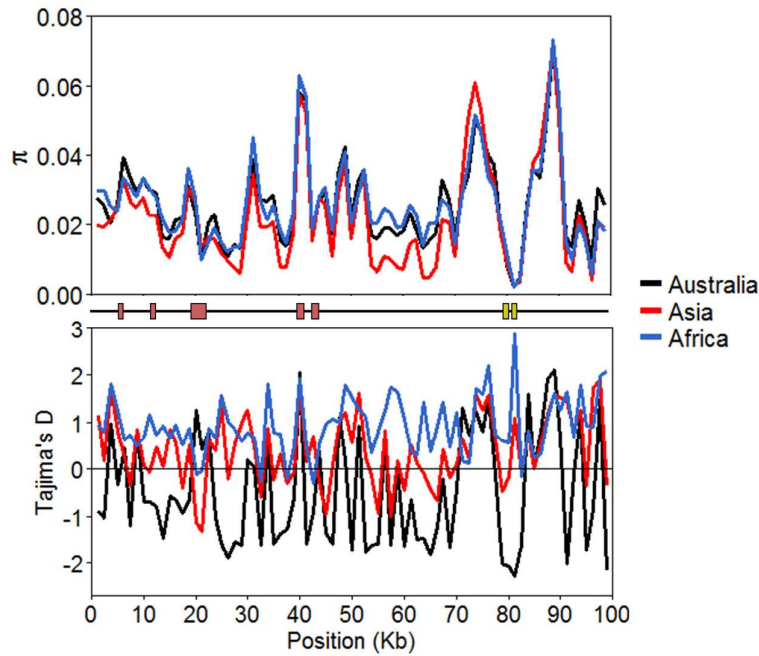
810

811

812

813

814 Fig. 9. Nucleotide diversity (π , top) and Tajima's D (bottom) calculated across sliding windows of the
815 33J17 BAC (JQ995292.1) for individuals found to be homozygous for haplotypes of the chimeric P450
816 gene associated with fenvalerate resistance. The location of gene bodies are indicated between the
817 plots, with those in red identified as potential reverse transcriptases and those in yellow as exons of
818 *CYP337B3v1*.



819